Polymer Testing 87 (2020) 106505

Contents lists available at ScienceDirect

Polymer Testing

journal homepage: http://www.elsevier.com/locate/polytest

Glass fiber reinforced bismaleimide/epoxy $BaTiO_3$ nano composites for high voltage applications

K. Savitha Unnikrishnan [a], T. Sunil Jose [a,*], S. Dinoop lal [a], K.J Arun [b]

[a] Department of Chemistry, St. Thomas' College (Autonomous), Thrissur, Kerala, 680001, India
[b] Department of Physics, Sree Kerala Varma College, Thrissur, Kerala, India

ARTICLE INFO

Keywords:
Bismaleimide
Epoxy
Composites
$BaTiO_3$ nanoparticles
Tensile strength
Flexural strength
Dielectric constant

ABSTRACT

$BaTiO_3$/bismaleimide/epoxy/glass fiber reinforced composites were prepared using E-glass fiber (E-GF) and silane coated E-glass fiber (SC-EGF) separately as reinforcement. $BaTiO_3$ nanoparticles were prepared by hydrothermal method. Results show that the addition of $BaTiO_3$ nanoparticles has significant effects on the mechanical and dielectric properties of the composite. Both E-GF and SC-EGF reinforced $BaTiO_3$/bismaleimide/epoxy composites with 2 wt percentages of $BaTiO_3$ nanoparticles showed improved tensile strength, flexural strength and dielectric constant and those with 3% showed high dielectric strength indicating this composition is more adaptable for high voltage insulating applications. Dielectric constants and dielectric loss of the fabricated nanocomposites have been obtained at higher frequencies (in GHz) by using Vector Network Analyser at room temperature and was found to be highest for the BMI-Epoxy nanocomposite with 1% weight nanofiller.

1. Introduction

Bismaleimide(BMI) is a high performance thermosetting polyimide and find applications in radar, spacewarecomposites, stealth areas, super capacitors, PCB etc. [1,2]. Unmodified BMI composites owing to high crosslinking density during curing are brittle in nature [3,4]. In order to overcome its brittleness, structural modifications, co-reactions, blending with suitable compounds, glass fiber or carbon fiber reinforcement are adopted. Epoxy resins are widely used as matrix materials for high performance composites. In order to enhance both the temperature performance and the processing ease, BMI is blended with epoxy resins [3,5–10]. High dielectric permittivity is highly desired for the dielectric materials used in the embedded capacitors and energy storage device [11–13]. In order to enhance the dielectric properties of BMI composites suitable nanofillers with high dielectric constants are added.

Dielectric properties of $BaTiO_3$ ceramics depend on the grain size. The $BaTiO_3$ with grain size 10 μm exhibits dielectric constant in the range of 1500–2000 at room temperature and those with grain size approximately 1 μm are capable of exhibiting dielectric constant in the range of 3500–6000 at room temperature, values as high as 15000 are possible for $BaTiO_3$ with nanosize [14]. To improve the mechanical properties of nanocomposite, glass fibers are reinforced into bismaleimide resin matrix via hand layup method and tested for dielectric properties and mechanical properties like tensile strength and flexular strength [15].

Morphological studies of the synthesized composite have been performed using SEM and structural studies using XRD-EDX, FT-IR. Dielectric constant, dielectric strength, dielectric loss factor and tan δ using LCR Meter, dielectric breakdown voltage (BDV) through I-V characteristics using Keithley high resistance meter, thermal stability using TGA and DSC [16,17].

This article focused on the effect of the influence of $BaTiO_3$ nanoparticles on the dielectric, mechanical and thermal properties of Bismaleimide – epoxy composites reinforced with glass fiber. $BaTiO_3$ nanoparticles were synthesized by hydrothermal method and characterized using Scanning Electron Microscopy (SEM) and Powder X-ray Diffraction (XRD). The synthesized $BaTiO_3$ nanoparticles were incorporated to Bismaleimide – epoxy matrix in varying percentages and the parameters were investigated.

2. Experimental

2.1. Materials

Bismaleimide powder resin was obtained from ABR Organics Ltd.,

* Corresponding author.
E-mail address: sjtppc@gmail.com (T. Sunil Jose).

https://doi.org/10.1016/j.polymertesting.2020.106505
Received 17 November 2019; Received in revised form 12 March 2020; Accepted 20 March 2020
Available online 26 March 2020

Table 1
Weight percentages of Bismaleimide-Epoxy- $BaTiO_3$ nanoparticles for composite preparation.

Code	Weight Ratio
BMI -Epoxy	15:1.5
BMI –Epoxy-BT-1	15:1.5: 0.165
BMI –Epoxy- BT-2	15:1.5: 0.33
BMI –Epoxy- BT-3	15:1.5: 0.66
BMI –Epoxy- BT-4	15:1.5: 1.32
BMI –Epoxy- BT-5	15:1.5:2.64

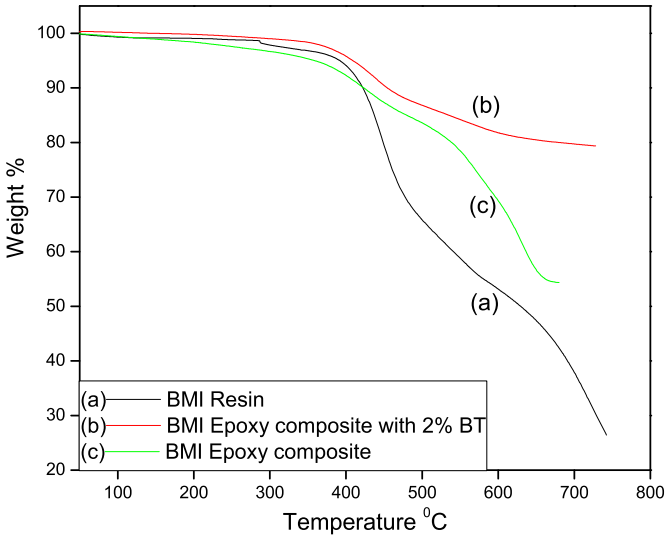

Fig. 1. TGA curves of (a) BMI resin (b) BMI Epoxy nanocomposite with 2% BT nanofiller(c) BMI Epoxy composite.

Table 2
Weight loss percentages of samples obtained from TGA curves.

Sample	Stage	Temperature in ^{0}C	Weight loss %	Total weight loss in %
BMI Resin	I	Up to 302	3	68
	II	375–467	23	
	III	470–575	20	
	IV	588–725	22	
BMI Epoxy Composite Without BT filler	I	Up to 301	No considerable weight loss	44
	II	302–398	5	
	III	400–563	17	
	IV	564–711	22	
BMI Epoxy Composite with (2%) BT nanofiller	I	Up to 320	No considerable weight loss	20
	II	332–423	5	
	III	424–570	10	
	IV	571–725	5	

Hyderabad. Epofine-1564 was purchased from Fine Finish Organics Pvt. Ltd., Taloja. E Glass fibres (E-GF) and Silane coated E Glass fibres (SC-EGF) from Urja Products Pvt. Ltd. India. Tetrabutyltitanate Ti $(C_4H_9O)_4$, Barium hydroxide octahydrate $Ba(OH)_2.8H_2O$, Nitric acid were purchased from Sigma Aldrich, India and were used as such without any further purification.

2.2. Preparation of $BaTiO_3$ (BT) nanoparticles

$BaTiO_3$ nanoparticles was synthesized by hydrothermal method from $Ti(C_4H_9O)_4$ and $Ba(OH)_2.8H_2O$ precursors [18–24]. Typically 1 ml of Ti

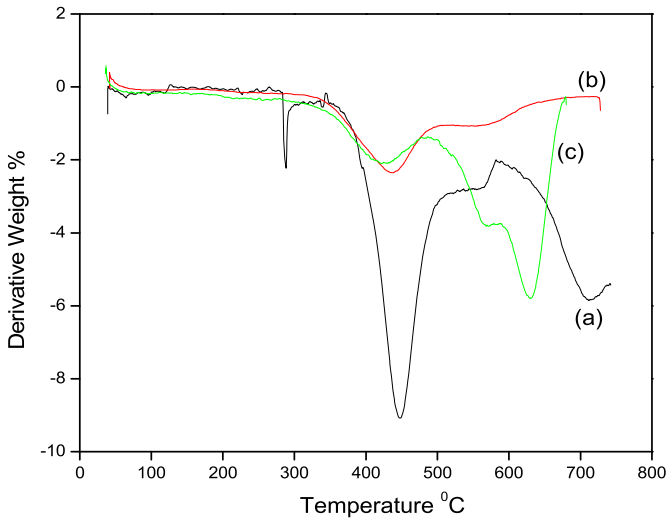

Fig. 2. DTG curves of (a) BMI resin(b) BMI Epoxy composite (c) BMI Epoxy nanocomposite with 2% BT nanofiller.

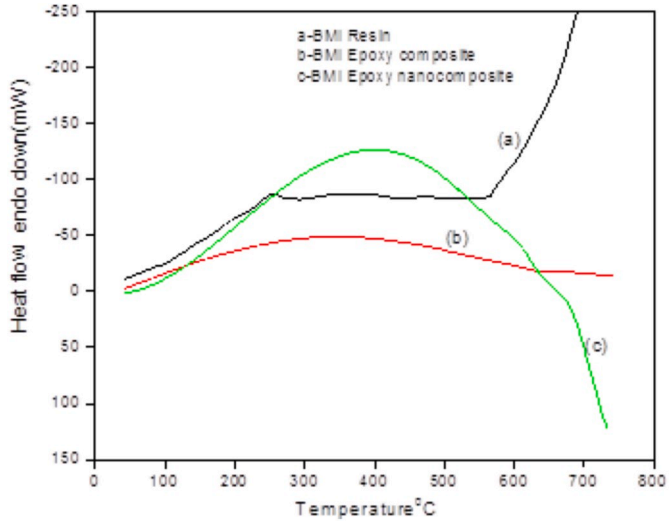

Fig. 3. DSC curves of (a) BMI resin powder (b) BMI Epoxy composite (c) BMI Epoxy nanocomposite with 2% BT nanofiller.

$(C_4H_9O)_4$ was added to18 ml ethanol solution in drops with continuous stirring. Slow addition of 0.06 ml HNO_3 and 3 ml distilled water was then followed. 10 ml of this freshly prepared solution was added dropwise into aqueous $Ba(OH)_2$ solution whose concentration was maintained at the range of 1.0 M, with continuous stirring. This mixture was transferred into a Teflon lined autoclave maintained at 200 °C and kept for 16 h. The autoclave was cooled to room temperature, products were filtered, washed with distilled water – ethanol mixture and dried at 60 °C under vacuum for 24 h [25].

2.3. Preparation of BMI-Epoxy composites

The conventional solvent method was inappropriate for the preparation of composites because the solvent DMF will not be able to evaporate completely and during evaporation blisters appear on the surface of composite. BMI and Epoxy resin containing $BaTiO_3$ nanoparticles in the ratio 15:1.5were mixed and ground well. Unidirectional E glass fiber is used as reinforcement. First glass fiber sheet is placed above resin nanoparticle matrix, uniformly pressed using Teflon rollers. It is repeated up to four layers. The different samples of glass reinforced

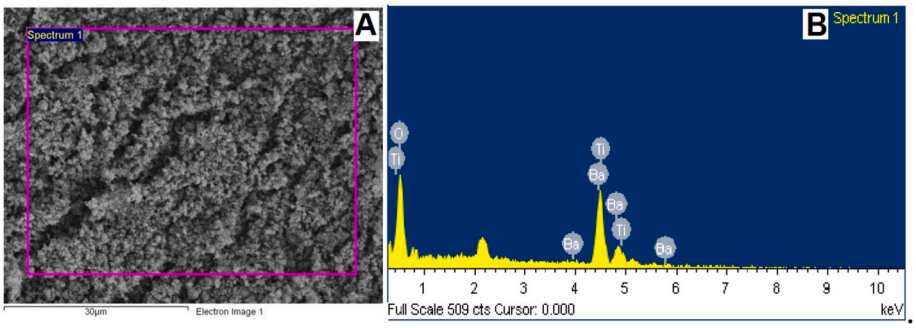

Fig. 4. SEM image (A) and EDAX (B) of $BaTiO_3$nanoparticles.

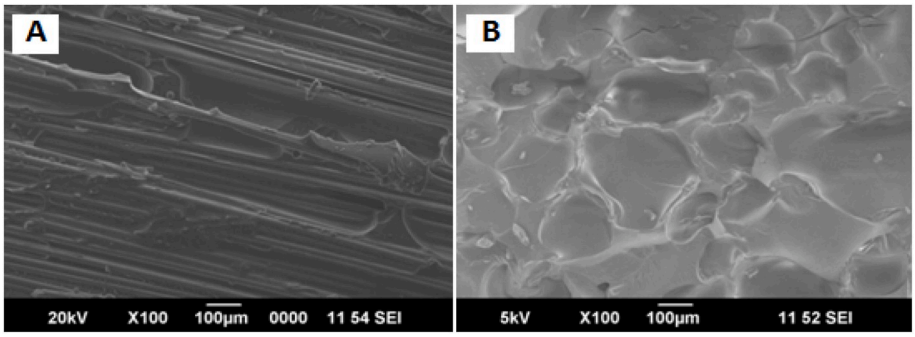

Fig. 5. SEM images of A) BMI epoxy composite B) BMI Resin.

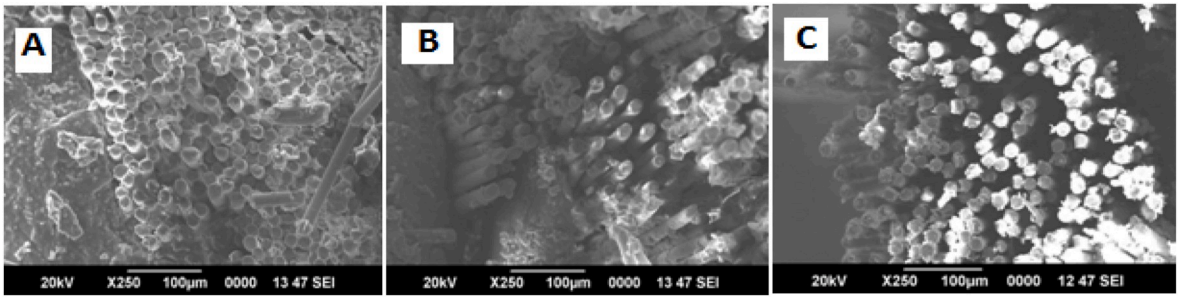

Fig. 6. Cross sectional SEM images of BMI epoxy nanocomposites with (A)1% (B)2% (C) 3% weights of BT nanoparticles.

Table 3
Weight and atomic percentages of various elements present in $BaTiO_3$ nanoparticles obtained from EDAX.

Element	Weight %	Atomic %
O K	17.46	55.05
Ti K	21.31	22.45
Ba L	61.23	22.50
Total	100	

$BMI/Epoxy/BaTiO_3$ nanocomposites were prepared by mixing the resin mixture with varying percentages of $BaTiO_3$ nanoparticles as mentioned in Table 1. Thus simple hand lay up method is used for the fabrication of glass fibre reinforced composites followed by compression moulding at 200 psi. The composite was kept in press at 100 °C for 10 min then raised to 120 °C for further 10 min, again raised to 140 °C for 10 min and finally for half hour at 180 °C [26–30]. The same procedure is adopted for the preparation of glass reinforced BMI-Epoxy composites without $BaTiO_3$ nanoparticles.

2.4. Measurements

Scanning Electron Microscopy (SEM) –EDAX of BMI, $BaTiO_3$, BMI/Epoxy composite and $BMI/Epoxy/BaTiO_3$ nanocomposite were obtained on ESEM Quanta 200 FEI from IISC Bangalore. Powder X-ray Diffraction (XRD) were recorded on Bruker AXS D8 Advance from CUSAT, Kochi to determine the morphology and composition of the synthesized $BaTiO_3$ [30–32]. FTIR spectra were recorded on IR Affinity-1S, Shimadzu from MES Keveeyem College, Valanchery. TGA and DTA measurements were carried out on PerkinElmer Diamond and DSC using Mettler Toledo DSC 822E from CUSAT, Kochi. Mechanical properties such as tensile strength and flexural strength of BMI-Epoxy composites were studied on 50 KN UTM-1205 from CBPST (CIPET), Kochi.

3. Results and discussion

3.1. Thermogravimetric analysis

TGA curves of cured BMI, BMI-Epoxy and BMI-Epoxy composite with 2% weight of BT nanofiller composites without glass fiber were obtained by thermogravimetric analyser apparatus at a heating rate of 20°C/min

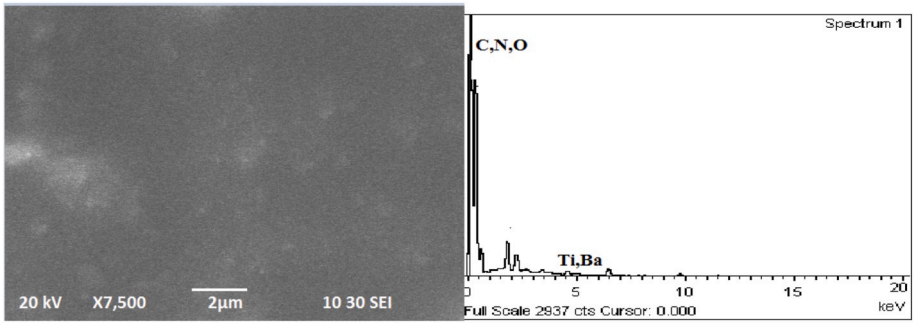

Fig. 7. SEM and EDX of BMI-Epoxy containing 2 wt % BT nanocomposite.

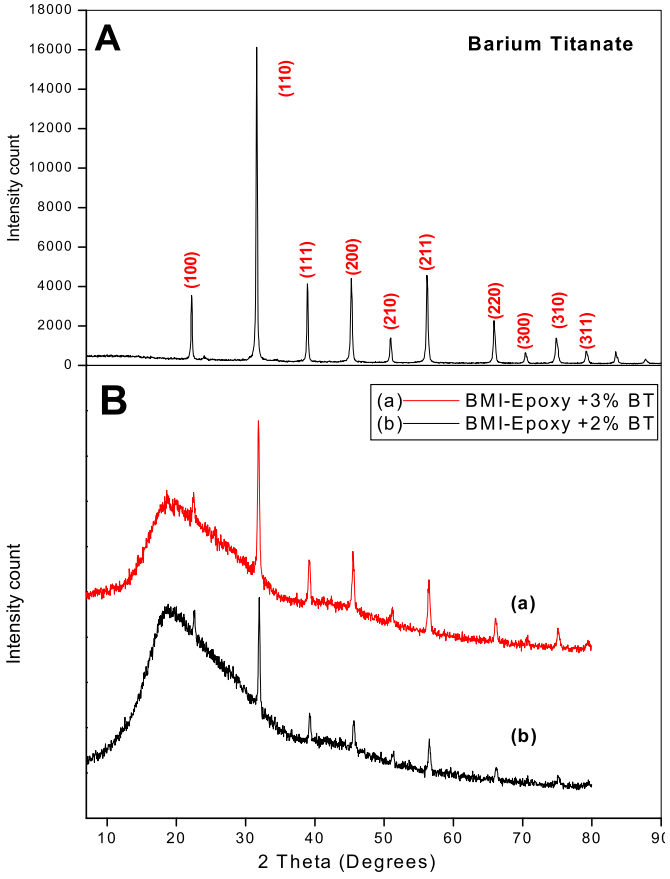

Fig. 8. X-ray Diffraction pattern of the (A) synthesized $BaTiO_3$ nanoparticles (B) (a) BMI-Epoxy 3%BT (b) BMI-Epoxy 2% BT.

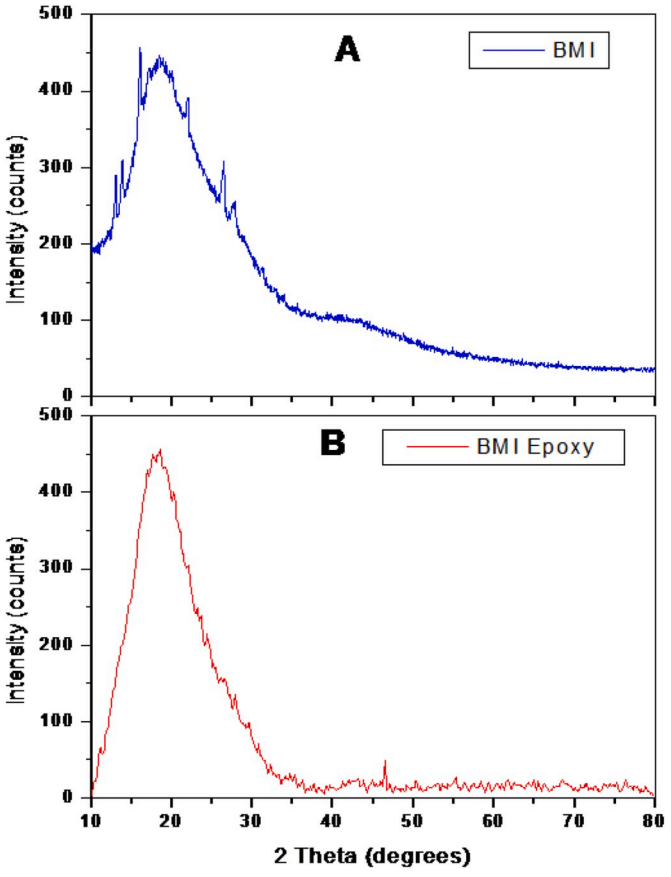

Fig. 9. X ray Diffraction pattern of (A) unmodified uncured neat BMI resin(B) BMI Epoxy composite.

from 40°C to 730°C. All sample weights remained less than 10 mg.(see Fig. 1)

From the TGA curves it is clear that BMI Epoxy composite with 2% BTis having higher thermal stability compared to BMI resin and BMI-Epoxy matrix that may be due to the interaction of the dispersed BT nanofiller with adjacent polymer matrix layers. The addition of thermally stable fillers can ensure not only good compatibility but also will improve the nano composite thermal stability due to their low migration characteristics [33].(see Table 2)

Curing is observed as a large exothermic peak. The exothermic peak temperature reflects the maximum rate of curing of the resin. By analyzing the DTG curves of cured BMI, BMI-Epoxy and BMI-Epoxy composite with 2% weight of BT nanofiller composites without glass fiber (Fig. 2), it is clear that exothermic peak temperature decrease from 446.83 C to 440.52 C in cured BMI Epoxy and to 421.60 C in the case of BMI Epoxy composite with 2% weight of BT nanofiller composites indicating that maximum rate of curing of resin decreases during the fabrication of BMI Epoxy composite with 2% weight of BT nanofiller composites without glass fibers.

Comparative analysis of the DSC curves of cured BMI (Fig. 3(a)), BMI Epoxy and BMI Epoxy composite with 2% weight of BT nanofiller we are getting peaks in negative direction for both BMI Epoxy and BMI Epoxy composite with 2% weight of BT nanofiller reveals they are undergoing crosslinking (Fig. 3(b) and (c). Among the above two BMI Epoxy composite with 2% weight of BT nanofiller has undergone more crosslinking. The DSC curve also confirms the Tg of Bismaleimide resin is at 288.85°C. Tg of BMI resin and BMI-Epoxycomposite with 2% weight of BT nanofiller were increased by the modification and addition of BT nanofiller [34]. In DSC broadened Tg is associated with an enhancement of tensile strength [35].

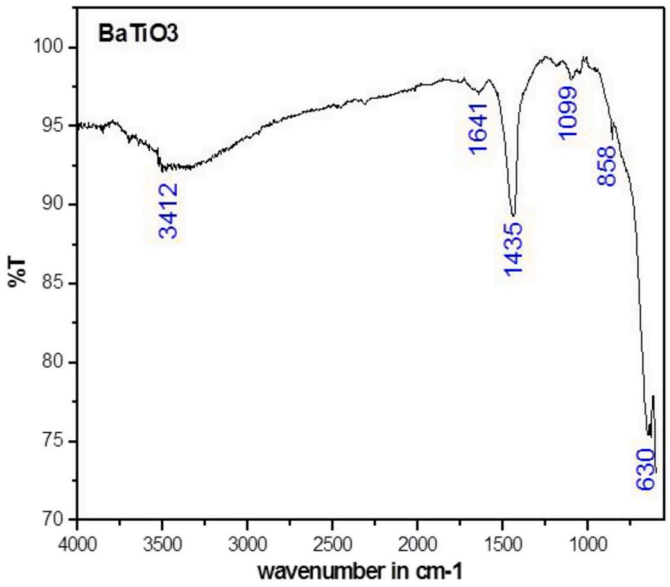

Fig. 10. FTIR Analysis of the synthesized $BaTiO_3$.

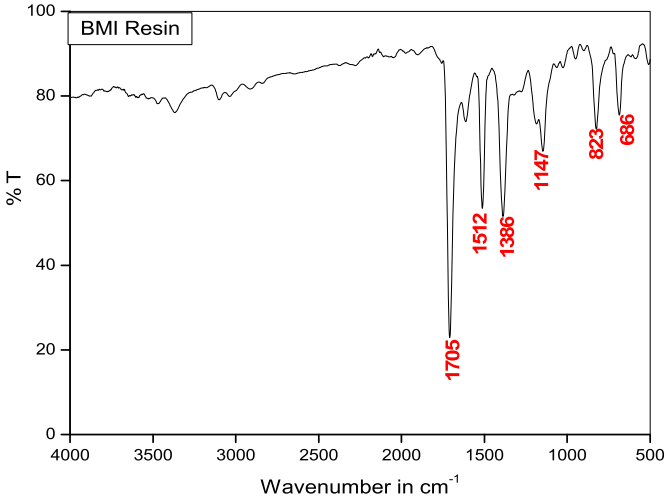

Fig. 11. FTIR Analysis of unmodified uncured BMI Resin.

3.2. Morphology of BMI epoxy nanocomposite

The morphology of $BaTiO_3$ nanoparticles Fig. 4(A), BMI epoxy composite (Fig. 5) and BMI epoxy nanocomposites(Fig. 6) has been studied by SEM.

Elemental Dispersive X-ray (EDAX) spectrum of the synthesized $BaTiO_3$ nanoparticles (Fig. 4B) confirms the formation of $BaTiO_3$ with compositions as Barium 55.05%, Titanium 22.45% and Oxygen 22.5% in the sample (Table 3).

From the SEM images of BMI-Epoxy BT composites BT nanoparticles (Fig. 7)are homogeneously dispersed throughout the polymer matrix and no agglomeration or voids are observed (see Fig. 5). Epoxy moiety can induce interaction with BMI resin via ring opening reaction. As a result, the distribution of nanofiller in the polymer matrix is enhanced which is important to obtain desired dielectric and thermal properties.

The highest tensile strength is observed in composite with 2% weight of the BT nanoparticles may be due to the uniform distribution of nanofiller in the Bismaleimide-epoxy matrix and less agglomeration of the nanofiller that facilitated the good interaction between the polymer matrix and nanofiller and are evident from SEM images (Fig. 7).

From EDX of BMI-Epoxy nanocomposite with 2% BT,we can see overlapped regions in the initial stage which indicates the presence of C (0.277),N(0.392),O(0.525)and Ti(0.39,0.452,0.5 & 4.51,4.5,4.9). We can see two small peaks between 4.5 and 5.0 which indicates the presence of both Ti and Ba. From this it is evident that the BT nanofillers are effectively dispersed in the polymer matrix.

3.3. X ray diffraction analysis

(a) X ray Diffraction analysis of $BaTiO_3$ nanoparticles

The analysis of XRD pattern matched with JCPDS No#892475. The most intense peak (110) is found at $2\theta = 31.57$. The peaks at $2\theta = 22.19$ (100), 31.57(110), 38.92(111), 45.27(200), 50.96(210), 56.18(211), 65.87(220), 70.39(300), 74.82(310) and 79.17(311) confirm the formation of perovskite structure of the synthesized BaTiO3 nanoparticles. Using Scherrer's formula, the average crystallite size of the $BaTiO_3$ nanoparticles is calculated and found to be 32.64 nm.

By comparing Fig. 8B (a) and 8B (b) with 9B, it is clear that the narrow diffraction peaks between 2θ ranges from 19 to 22 is retained at XRD patterns of both BMI Epoxy composites with and without BT nanofiller. Further analysis of Fig. 8(B) (a) and (b) reveals that 2θ values of most intense peak (110) is not that much changed and peaks at 110,111,200,210,211,220 and 310 are also seen in both BMI Epoxy composites with 2% and 3% BT nanofiller confirming the effective dispersion of BT nanofiller.

(b) X-ray Diffraction analysis of BMI Resin

The X-ray diffraction pattern of the unmodified uncured neat BMI resin (Fig. 9A) shown below exhibits its characteristic peaks at $2\theta =$ 12.86, 13.76, 15.86, 21.96, 26.29 and 27.75. The sharp narrow diffraction peaks between 2θ ranges 10 to 30 could explain the brittle nature of the resin. The sharp narrow diffraction peaks corresponds to the crystalline regions while broad peaks corresponds to the amorphous regions of the resin. The presence of crystalline regions resulted in the brittleness of the resin [36]. XRD pattern of BMI Epoxy composite [Fig. 6 (B)] confirms that addition of epoxy resin decreases the brittle nature of the resin.

3.4. FTIR analysis

FTIR spectra of $BaTiO_3$ exhibited peaks at 630 and 868 cm^{-1} corresponding to the metal-oxygen (Ti-O) stretching vibrations. Peaks at 1641 and 3412 cm^{-1} corresponded to the –OH deformation and stretching vibrations due to the presence of adsorbed –OH group. A weak absorption peak at 1641 cm^{-1} attributed to the bending vibration of H-*O*-H arose from adsorbed water molecules. A strong peak at 1436 cm^{-1} is related to C-O stretching vibration arose from the trace of $BaCO_3$ present in $BaTiO_3$ (Fig. 10)[37].

From the ATR FT-IR spectra of the uncured BMI resin (Fig. 11) and the cured BMI/Epoxy nanocomposites, it can be seen that the strong absorption band at 1147 cm^{-1} attributes to the maleimide C-N-C stretching vibration disappeared during curing, indicating the conversion of maleimide functionality. The characteristic absorption peak of the imides are at 1705 cm^{-1}(+or – 10 cm^{-1}), in all the cured BMI/Epoxy composites and the uncured BMI resin there exists a strong absorption peak at 1705 cm^{-1} indicating the presence of strong C=O asymmetric stretching. At 2341 cm^{-1} and 2320 cm^{-1} peak of atmospheric CO_2 due to asymmetric stretching mode of gas phase CO_2 was found.

The strong absorption bands due C-N-C and C-N stretching were observed at 1512 cm^{-1} and 1386 cm^{-1}. Characteristic absorptions due to the maleimide ring observed at 686 cm^{-1}, 823 cm^{-1}, 1147 cm^{-1}, 1386 cm^{-1} and C=C stretch was observed at 1510 cm^{-1}. Analysis and comparison of the FT-IR absorption spectrum of the cured composites and the uncured BMI resin showed reduced number of peaks in the range of 600–1600 cm^{-1} indicating the completion of curing of BMI resin [36,

Table 4
The tentative assignment of the main absorption bands of FT-IR.

Uncured BMI	BMI Epoxy nano composites					Tendative assignment
	1%	2%	3%	4%	5%	
3471 (Somewhat strong peak)	3495 3392 medium	3396 Very weak	3533	3475 3518 Very weak	3496 3518	Presence Of –OH group
686	680	680	680	682	682	Presence of Maleimide benzene
1386	1382	1382	1384	1384	1384	Ring and imide group
1705 (very strong)	1705 strong	1705 strong	1705 strong	1705 strong	1705 Strong	Presence of C=O group
1512 (strong)	1510 (strong)	1512	1512	1512 (strong)	1512 (strong)	C=C Benzene ring
1147 (strong)	1149 weak	1143 Very weak	Very Weak Hard to find	Very Weak Hard to find	1095	-C-N-C Maleimide group
823 strong	806 strong	808 medium	800 medium	800 strong	798 strong	Benzene ring
950 medium	946 Very weak	941 weak	Very Weak Hard to find	Very Weak Hard to find	Very Weak Hard to find	Benzene ring
3101 medium	3101 Very weak	Very Weak Hard to find	Very Weak Hard to find	3109 weak	2956 weak	-CH-Maleimide
1613medium	157Very weak	1610 Weak	1623 Weak	1521medium	1595 weak 1510medium	Epoxy
1024 weak	1020 Weak	1025 weak	Very Weak Hard to find	Very Weak Hard to find	1110 weak	Weak C-N-Stretch

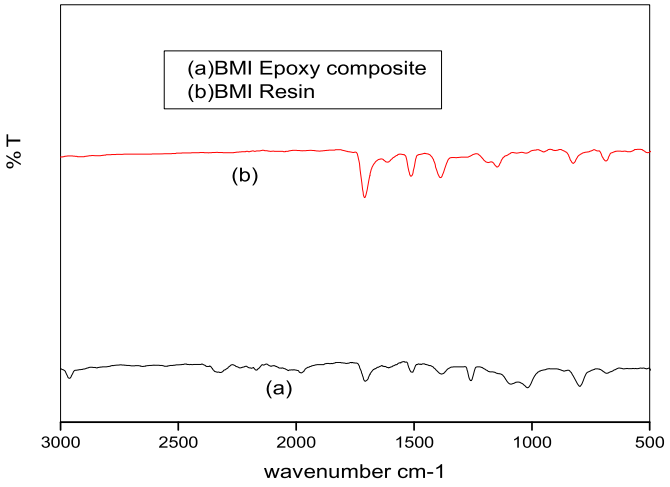

Fig. 12. FTIR Analysis of (a)BMI Epoxy composite(*b*)unmodified uncured BMI Resin.

38] (see Table 4).

FTIR spectra of E-GF and SC-EGF reinforced BMI-Epoxy composites with varying weight percentages (1–5%) are shown in Fig. 13. Comparative studies reveal that the characteristics peaks are not that much altered in differently reinforced BMI-Epoxy BT nanocomposites. The characteristic absorption peak of the imides at 1705 cm^{-1}, the C=C stretching of aromatic rings 1603-1613 cm^{-1} in epoxy, C-C stretching of aromatic ring at 1509 cm^{-1} are retained in both FTIR spectra. In the FTIR spectra of E-GF reinforced BMI-Epoxy nanocomposites, small peak between 2873 and 2965 cm^{-1} has been observed which is due to the

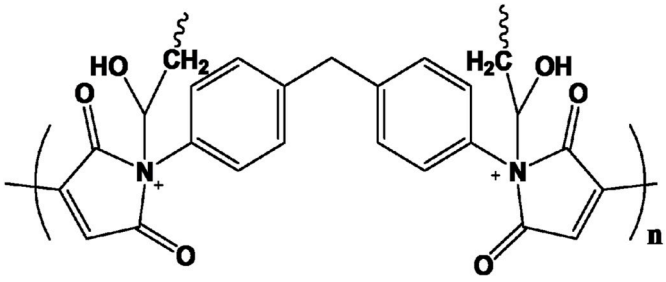

Fig. 14. Intercrosslinking between BMI and epoxy resin.

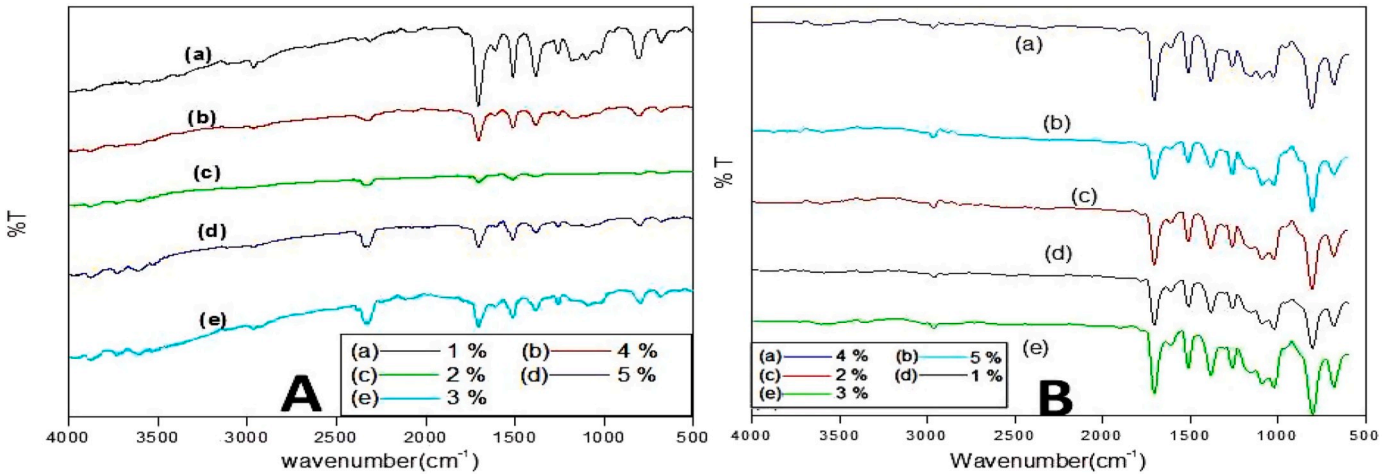

Fig. 13. FTIR Analysis of the BMI Epoxy nanocomposites reinforced with (A) E –GF (B) SC - EGF.

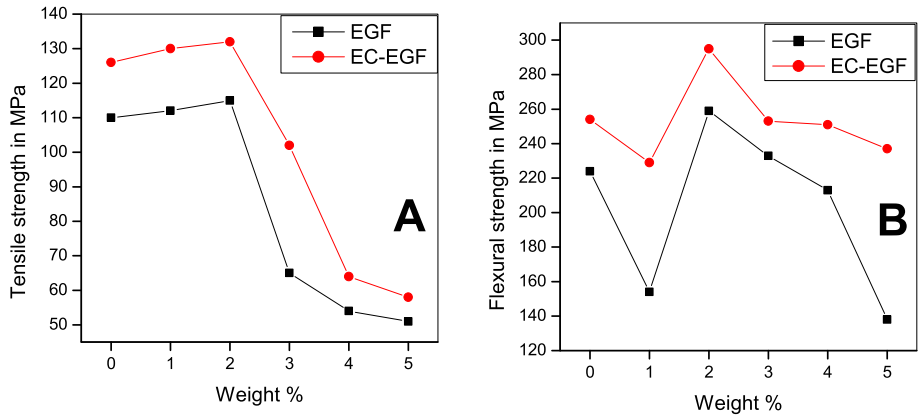

Fig. 15. (A) and (B)-comparitive study of effect of weight % of $BaTiO_3$ nanoparticles on tensile strength and flexural strength of the composites reinforced with E-glass fiber (EGF) and Silane coated E-glass fiber(SC- EGF).

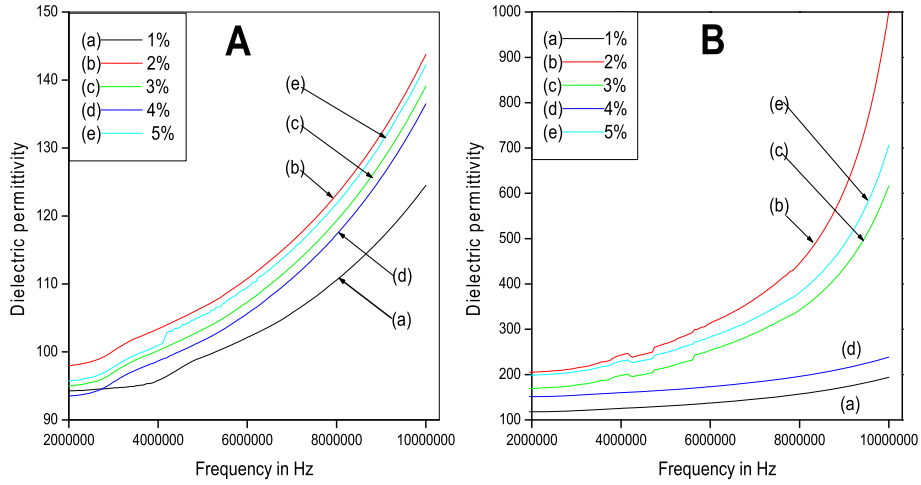

Fig. 16. Frequency –dielectric permittivity graph of BMI epoxy nanocomposites reinforced with (A) E-GF (B)SC-EGF.

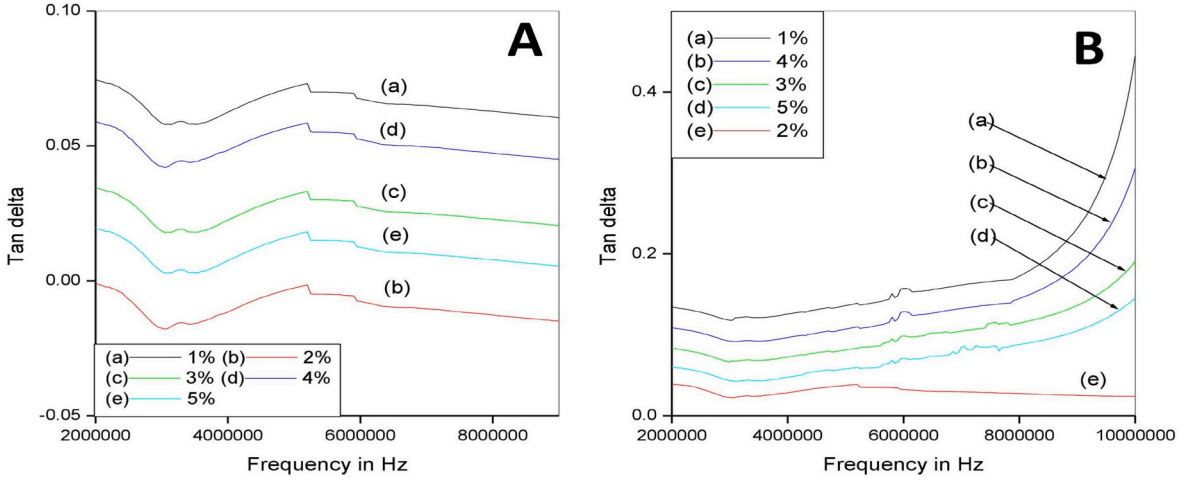

Fig. 17. Frequency -tan δ graph of BMI epoxy composites reinforced with (A) E-GF (B) SC-EGF.

stretching of C-H of CH_2 and C-H aromatic and aliphatic. More intense peaks are observed in FTIR spectra of SC-EGF reinforced BMI-epoxy nanocomposites.

The IR peak for the oxirane ring of the epoxy resin is absent at 915 cm^{-1} in both BMI-Epoxy composites with and without nanofiller(Fig. 12 and 13). This suggests the possibility of ring opening and consequent crosslinking between epoxy and BMI. The appearance of OH peak beyond 3500 cm^{-1}due to the opening of the oxirane ring of the epoxy is found in all the BMI-Epoxy nanocomposites (Fig. 13) that indicates intercross linking between BMI and epoxy resin which proceeds through the ring opening of epoxy (oxirane ring) and formation of -N-CH(OH) CH_2- bonds between N of maleimide ring and –CH of epoxy resin

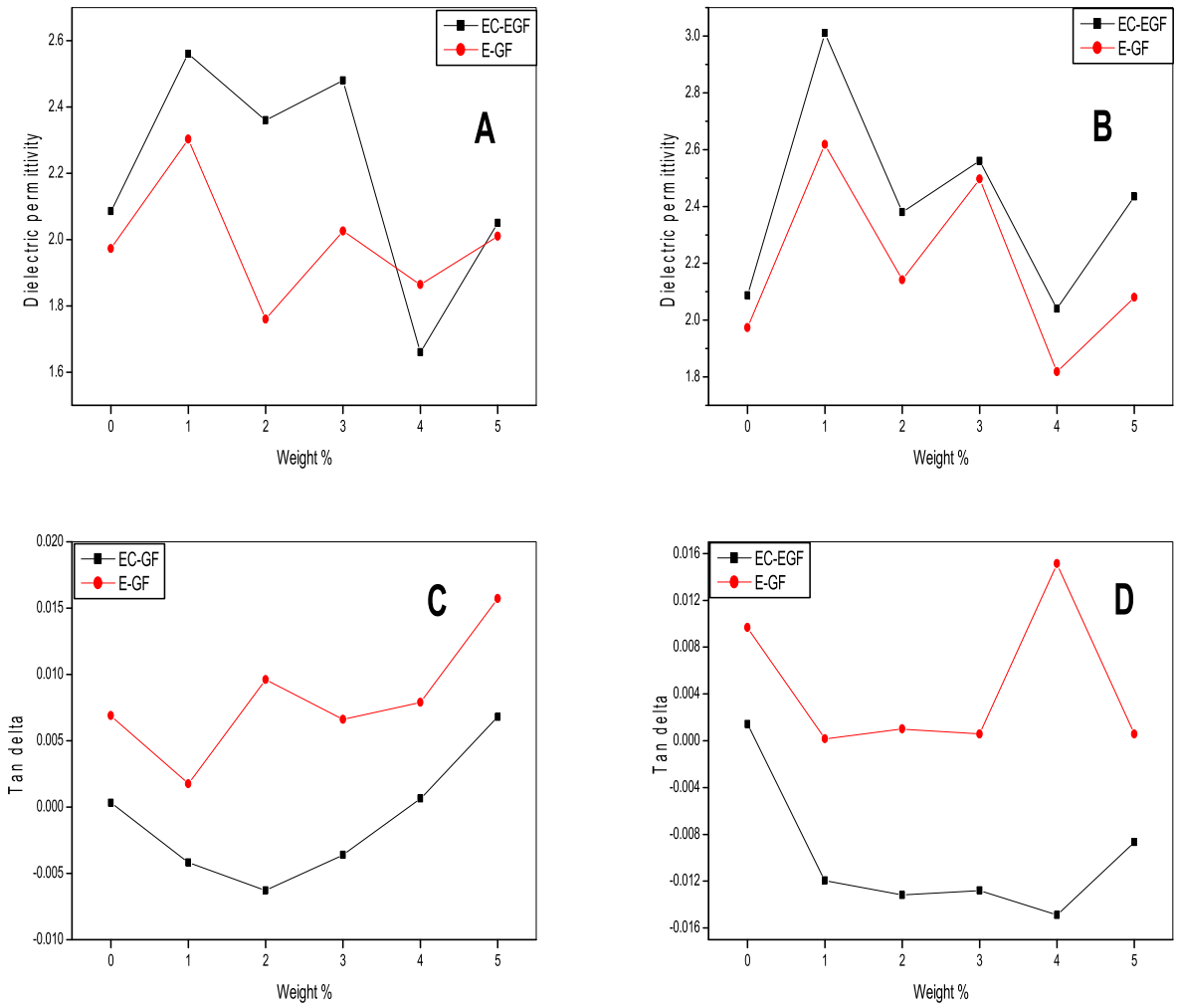

Fig. 18. Weight percentage–dielectric permittivity graph (A & B) and weight percentage-tan delta graph (C & D)of BMI epoxy nanocomposites with EGF and with SC-EGF at frequencies.

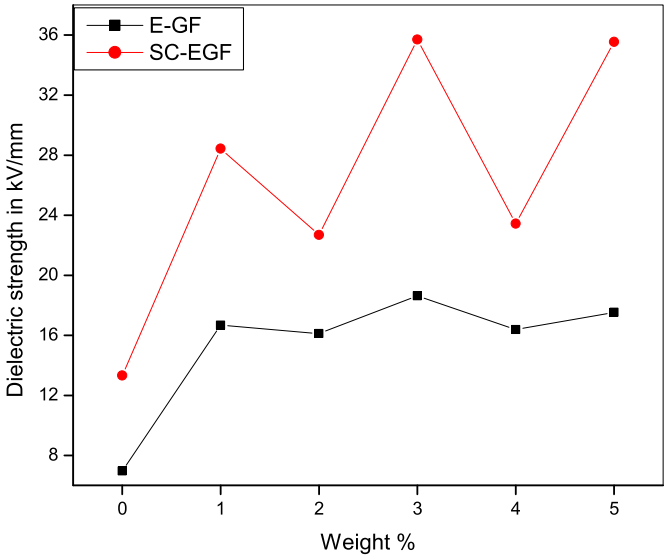

Fig. 19. Effect of weight percentage of $BaTiO_3$ nanoparticles of BMI epoxy composites on break down voltage.

(Fig. 14).

3.5. *Mechanical properties of BMI epoxy nanocomposite*

The flexural and tensile strength measurements were studied as per ASTM standards. The flexural and tensile strength of BMI epoxy nanocomposites (Fig. 15) are higher than that of BMI epoxy composite whose flexural strength and tensile strength are 224 Mpa and 110 Mpa respectively. For samples of BMI/BT-1 to BMI/Epoxy-BT-5 the flexural strength and tensile strength change when the ratio of $BaTiO_3$ nanoparticles are different and maximum value obtained when the percentage of $BaTiO_3$ nanoparticle is 2%.

The comparative analysis of the above test results showed that there is remarkable increase in the tensile strength and flexural strength of Silane coated E-glass fiber reinforced nanocomposite, establishing the fact that there exists greater interaction between Silane coated E-glass fiber and the matrix [39]. The tensile and flexural strength increases first and the decreases with the increase in weight % of the nanofiller. The increased rigidity contributed by the loaded nanofiller owing to the increased matrix to filler interaction is responsible for the enhanced tensile and flexural strength. When the weight % of the nanofiller is above a certain value, there is chance for filler agglomeration that may hinder the interchain interactions during the curing process and this result in decreased tensile and flexural strength.

3.6. Dielectric properties of the nanocomposites

3.6.1. Dielectric permittivity

Fig. 16 depicts the dependence of dielectric permittivity of BMI epoxy nanocomposite on the weight percentage of $BaTiO_3$ nanoparticles measured at room temperature at frequency range 10^1–10^7 Hz. Also with gradual increase in the ratio of $BaTiO_3$ nanoparticles, dielectric permittivity also increases gradually. The dielectric permittivity reached to maximum value when the weight percentage of $BaTiO_3$ nanoparticles was 2% in the case of BMI epoxy nanocomposites reinforced with E-GF and 2% in the case of BMI epoxy nanocomposites reinforced with SC-EGF

Dielectric permittivity usually decreases with increase in the frequency which is ascribed to an interfacial relaxation. Here the increased permittivity with increase in frequency may be attributed to either interfacial polarization or because of breakage of certain bonds at higher frequency or because of both effects.

(1) **Interfacial polarization** - Nanofiller content is responsible for the heterogeneity of the systems and the extended interface. Space charges migrate under the influence of the field and accumulated at the interfaces where they form dipoles with enhanced inertia. This charge trapping procedure at the interface contributes to the dielectric response and permittivity [40].

Interfacial polarization had no time enough to orient themselves in the direction of the alternating field [41].

(2) **Bond Breakage** – With increase in frequency, there is possibility for the breakage of bonds under severe oscillation resulting in the formation of charge centres in the matrix. So with increase in frequency, the extent of bond breakage also increases leading to increased permittivity.

3.6.2. Dielectric loss

Electrical conductivity, dielectric polarization etc. mainly depends on loss tangent or tan δ.

Due to high polarization of $BaTiO_3$ nanoparticles compared to that of BMI/Epoxy matrix, increase of dielectric permittivity was observed. By increasing the ratio of the $BaTiO_3$ nanoparticles, no trends can be seen in the values of the dielectric loss of the composites (Fig. 17). At very small ratio of $BaTiO_3$ (2%) the dielectric loss of the composite remained very low. The BMI epoxy nanocomposites have attracted much attention in practical applications due to its high dielectric permittivity and low dielectric loss.

3.6.3. Dielectric properties of the nanocomposites at high frequencies

Dielectric constants and dielectric loss of the fabricated nanocomposites have been obtained at higher frequencies (in GHz) by using Vector Network Analyser at room temperature and was found to be highest for the BMI-Epoxy nanocomposite with 1% weight nanofiller [42]. Dielectric permittivity depends on thickness of the sample, uniformity of the surface of the sample, presence of air occupied voids etc. So the measured values can change according to the variation in the above factors. We are getting negative delta values in some samples that may due to the above factors.(see Fig. 18)

3.6.4. Break down voltage and dielectric strength

The energy storage capacity and energy density of polymer nanocomposites depend upon the value of break down field strength. The AC Break down studies are performed on BMI/Epoxynanocomposites as per ASTM D149. Break down voltage varies with the material composition, shape of the material and the length of the material between the electrical contacts..(see Fig. 19)

4. Conclusions

Glass fiber reinforced Bismaleimide/Epoxy composite and Bismaleimide/Epoxy nanocomposite with $BaTiO_3$ nanoparticles at different filler loadings have been prepared. The effect of $BaTiO_3$ nanoparticles on the mechanical, thermal and dielectric properties of Bismaleimide/Epoxy composites was studied. Both Glass fiber reinforced (E-GF & SC-EGF)BMI/Epoxy/$BaTiO_3$ nanoparticles with 3% of $BaTiO_3$ have better insulating properties and with 2% exhibits better mechanical properties. Dielectric constants and dielectric loss of the fabricated nanocomposites have been obtained at higher frequencies (in GHz) by using Vector Network Analyser at room temperature and was found to be highest for the BMI-Epoxy nanocomposite with 1% weight nanofiller.

Declaration of competing of interest

Authors have no conflict of interest.

CRediT authorship contribution statement

K. Savitha Unnikrishnan: Conceptualization, Methodology, Data curation, Writing - original draft, Software, Visualization, Investigation, Project administration, Resources. **T. Sunil Jose:** Supervision, Writing - review & editing, Validation, Project administration, Resources. **S. Dinoop lal:** Writing - review & editing, Software. **K.J Arun:** Formal analysis.

Appendix A. Supplementary data

Supplementary data to this article can be found online at https://doi.org/10.1016/j.polymertesting.2020.106505.

References

[1] J. Hu, A. Gu, G. Liang, D. Zhuo, L. Yuan, Preparation and properties of mesoporous silica/bismaleimide/diallylbisphenol composites with improved thermal stability, mechanical and dielectric properties, Express Polym. Lett. 5 (6) (2011) 555–568.
[2] H.H. Wenhui Xu, Y. ding, S. Jiang, Y. Wan, X. Liao, High permittivity nanocomposites fabricated from electrospun polyimide/BaTiO3 hybrid nanofibers, Polym. Compos. (Mar 2016) 794–801.
[3] L. Jin, T. Agag, H. Ishida, Bis(benzoxazine-maleimide)s as a novel class of high performance resin: synthesis and properties, Eur. Polym. J. 46 (2) (2010) 354–363.
[4] G. Lu, Y. Huang, Preparation and Characterization of Bismaleimide Resin/titania Nanocomposites via Sol-Gel Process, 2013 *arXiv Prepr. arXiv1304.7082*.
[5] G. Horst Stenzenberger, Technochemie GmbH, "6-Bismaleimide-Resins.pdf.".
[6] L. Rajabi, V. Scientist, G. Malekzadeh, Effects of Bismaleimide Resin on Dielectric and Dynamic Mechanical Properties of Epoxy-Based Laminate, no, May 2006, 2014.
[7] K.P.O. Mahesh, M. Alagar, R.S. Kumar, Synthesis and characterization of polyurethane-toughened epoxy-bismaleimide matrices, High Perform. Polym. 16 (3) (2004) 391–404.
[8] R. Chandra, L. Rajabi, Recent advances in bismaleimides and epoxy-imide/bismaleimide formulations and composites, J. Macromol. Sci. Rev. Macromol. Chem. Phys. 37 (1) (1997) 61–96.
[9] K. Akiyama, K. Makino, C Syro-C Conse vols. 3–5, 1973.
[10] B.A. Rozenberg, E.A. Dzhavadyan, R. Morgan, E. Shin, High-performance bismaleimide matrices: cure kinetics and mechanism, Polym. Adv. Technol. 13 (10–12) (2002) 837–844.
[11] N. Phougat, P. Vasudevan, H.S. Nalwa, Handbook of Low and High Dielectric Constant Materials and Their Applications, vol. 1, 1999.
[12] P. Paper, Energy Storage Sys.for 22 (5) (2006), 31033.
[13] A. Gu, High performance bismaleimide/cyanate ester hybrid polymer networks with excellent dielectric properties, Compos. Sci. Technol. 66 (11–12) (2006) 1749–1755.
[14] P. Barber, et al., Polymer Composite and Nanocomposite Dielectric Materials for Pulse Power Energy Storage, vol. 2, 2009, 4.
[15] R. Chandra, L. Rajabi, Recent advances in bismaleimides and epoxy-lmide/bismaleimide formulations and composites, J. Macromol. Sci. Polym. Rev. 37 (1) (1997) 61–96.
[16] T.M. Donnellan, D. Roylance, 18974, Development Center Warminster, Pennsylvania, 32, 1992, pp. 5–10, 6.
[17] H. Zheng, K. Zhu, Q. Wu, J. Liu, J. Qiu, Preparation and characterization of monodispersed BaTiO3 nanocrystals by sol-hydrothemal method, J. Cryst. Growth 363 (2013) 300–307.
[18] Y. Mao, H. Zhou, S.S. Wong, Synthesis, properties, and applications of perovskite-phase metal oxide nanostructures, Mater. Matters 5 (2) (2010) 50–53.

[19] A. Kareiva, S. Tautkus, R. Rapalaviciute, J.E. Jørgensen, B. Lundtoft, Sol-gel synthesis and characterization of barium titanate powders, J. Mater. Sci. 34 (19) (1999) 4853–4857.
[20] T. Batio, Structure and dielectric properties of perovskite, Structure (2002) 1–15.
[21] M. Gromada, M. Biglar, T. Trzepieciński, F. Stachowicz, Characterization of BaTiO3piezoelectric perovskite material for multilayer actuators, Bull. Mater. Sci. 40 (4) (2017) 759–771.
[22] J.H. Park, et al., Synthesis, structure and dielectric properties of BaTiO3nanoparticles, J. Kor. Phys. Soc. 49 (SUPPL. 2) (2006) 680–683.
[23] E.K. Al-Shakarchi, N.B. Mahmood, Three techniques used to produce $BaTiO_3$ fine powder, J. Mod. Phys. 2 (11) (2011) 1420–1428.
[24] C. Zheng, B. Cui, Q. You, Z. Chang, "Characterization of BaTiO 3 powders and ceramics prepared using the sol – gel process , with triton X-100 used as a surfactant, Sci. Res. (2010) 341–346.
[25] H. Zheng, K. Zhu, Q. Wu, J. Liu, J. Qiu, Preparation and characterization of monodispersed BaTiO3nanocrystals by sol-hydrothemal method, J. Cryst. Growth 363 (2013) 300–307.
[26] J.X. Lei, X.L. Liu, J.F. Chen, Hydrothermal synthesis and structure characterization of nanocrystalline barium titanate powders, Adv. Mater. Res. 11–12 (2006) 23–26.
[27] Z. Lazarević, et al., Characterization of barium titanate ceramic powders by Raman spectroscopy, Acta Phys. Pol., A 115 (4) (2009) 808–810.
[28] K.I. Osman, Synthesis and Characterization of BaTiO3 Ferroelectric Material, UniMAP vol. 176 (2011).
[29] T. Agag, T. Takeichi, Preparation, characterization, and polymerization of maleimidobenzoxazine monomers as a novel class of thermosetting resins, J. Polym. Sci. Part A Polym. Chem. 44 (4) (2006) 1424–1435.
[30] F. Huang, F. Huang, Y. Zhou, L. Du, Preparation and properties of bismaleimide resins modified with hydrogen silsesquioxane and dipropargyl ether and their composites, Polym. J. 42 (3) (2010) 261–267.
[31] Q. Yuan, F. Huang, Y. Jiao, Characterization of modified bismaleimide resin, J. Appl. Polym. Sci. 62 (3) (1996) 459–464.
[32] S. Vinayagamoorthi, C.T. Vijayakumar, S. Alam, S. Nanjundan, Structural aspects of high temperature thermosets - bismaleimide/propargyl terminated resin system-polymerization and degradation studies, Eur. Polym. J. 45 (4) (2009) 1217–1231.
[33] C.E. Corcione, M. Frigione, Characterization of Nanocomposites by Thermal Analysis, 2012, pp. 2960–2980.
[34] K. Ohtsuka, H. Kimura, S. Ikeshita, Novel Bismaleimide/Diallylbisphenol A Resin Modified with Multifunctional Thiol Containing Isocyanuric Ring and Long-Chain Aliphatic Unit vol. 28, 2016, pp. 591–599, 5.
[35] B. Pukanszky, Polymer/Lignin Blends : Interactions , Properties , Applications, 2017. October.
[36] S. Chandran M, M. Krishna, K. Salini, K.S. Rai, Preparation and characterization of chain-extended bismaleimide/carbon fibre composites, Int. J. Polym. Sci. 2010 (July, 2010).
[37] T.T.M. Phan, et al., Enhancement of polarization property of silane-modified BaTiO3nanoparticles and its effect in increasing dielectric property of epoxy/BaTiO3nanocomposites, J. Sci. Adv. Mater. Dev. 1 (1) (2016) 90–97.
[38] T. Procedure, "Chapter-5 Bismaleimide-Allyl Novolac Oligomers: Synthesis and Cure Kinetics," pp. 99–123.
[39] S.Y. Kanag, Y.K. Anandan, P. Vaidyanath, P. Baskar, Strength properties of coated E-glass fibres in concrete, Gradjevinar 68 (9) (2016) 697–703.
[40] G.C. Manika, G.C. Psarras, Barium Titanate/Epoxy Resin Composite Nanodielectrics as Compact Capacitive Energy Storing Systems vol. 13, 2019, pp. 749–758, 8.
[41] L. Wan, X. Zhang, G. Wu, A. Feng, Thermal Conductivity and Dielectric Properties of Bismaleimide/Cyanate Ester Copolymer vol. 2, 2017, pp. 167–171.
[42] S.P. Chakyar, S.K. Simon, C. Bindu, J. Andrews, V.P. Joseph, Complex permittivity measurement using metamaterial split ring resonators, J. Appl. Phys. 121 (5) (2017).